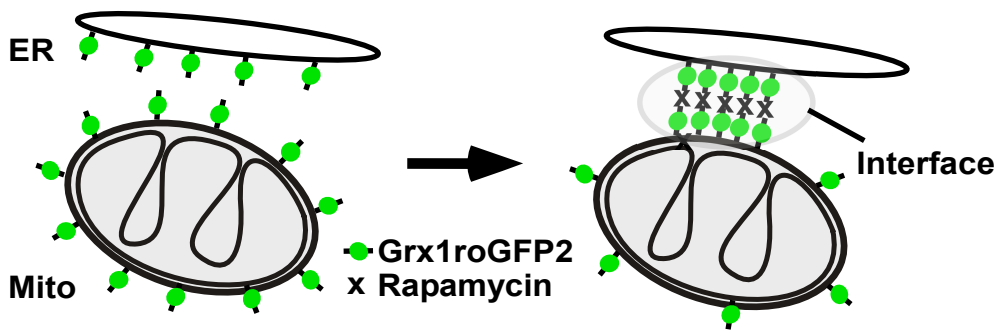
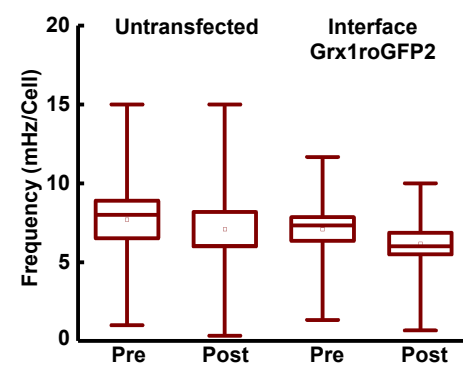
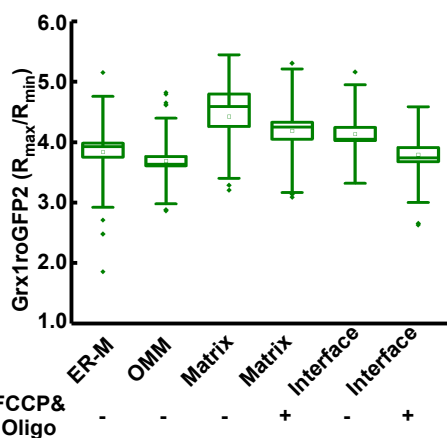
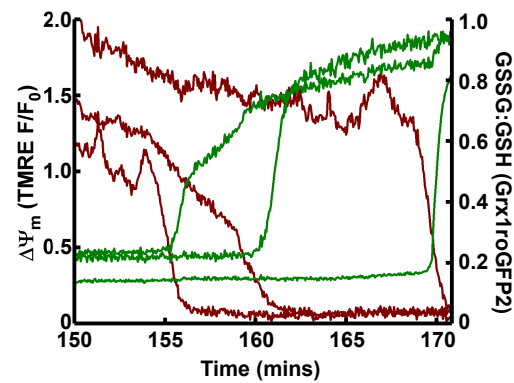
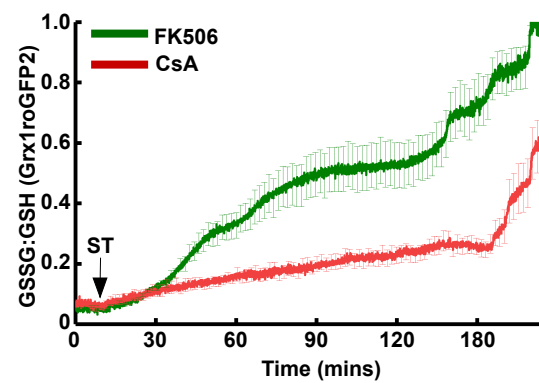
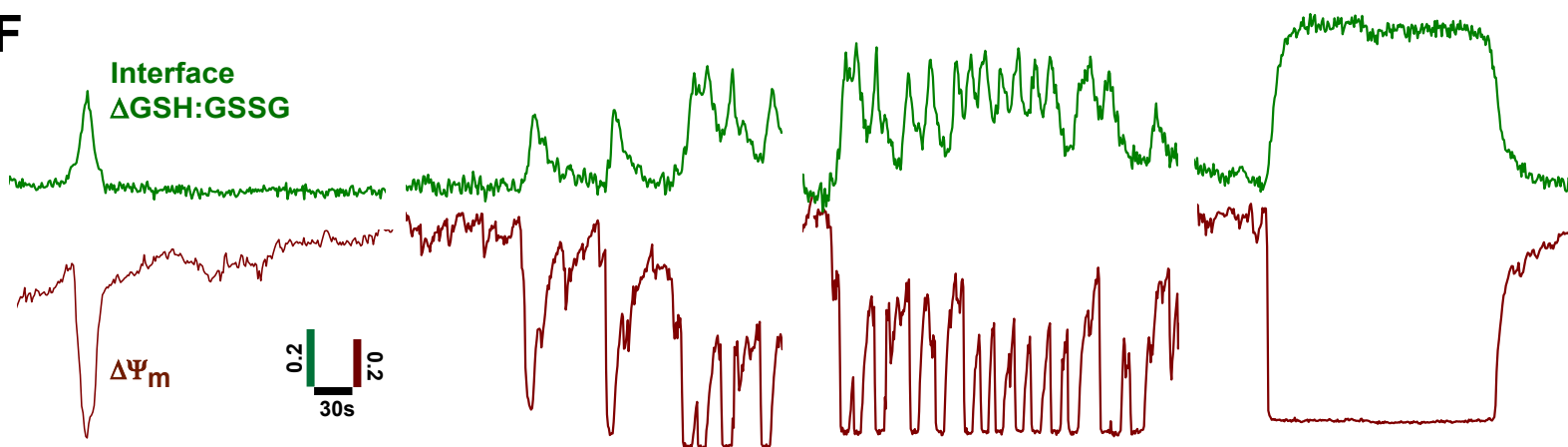
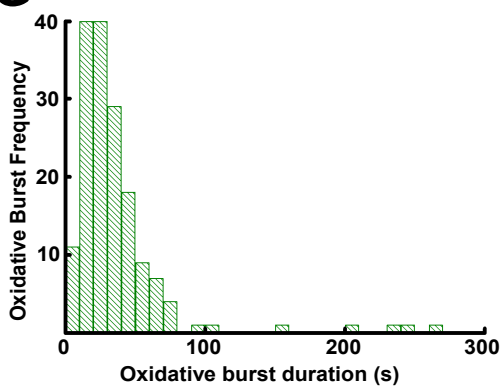
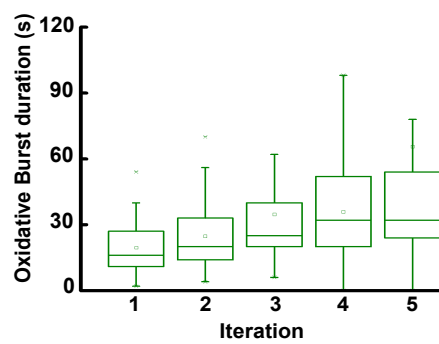
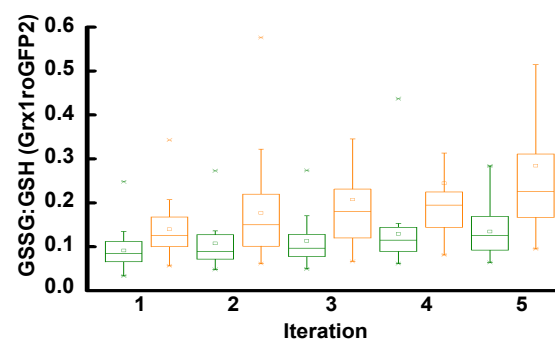
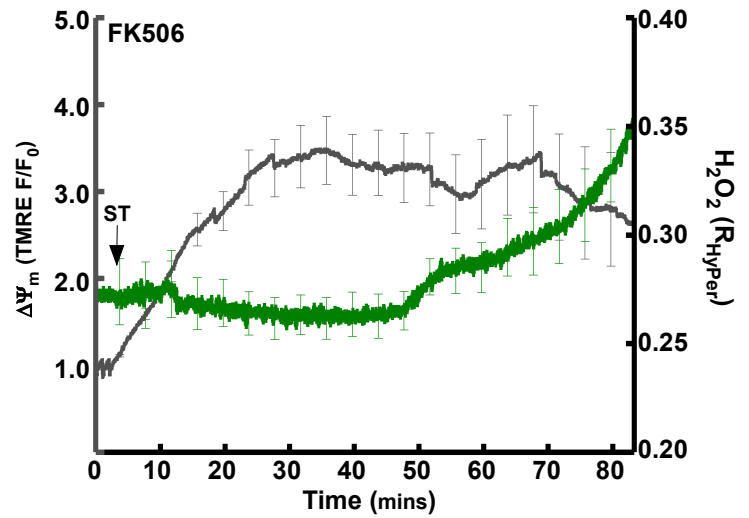
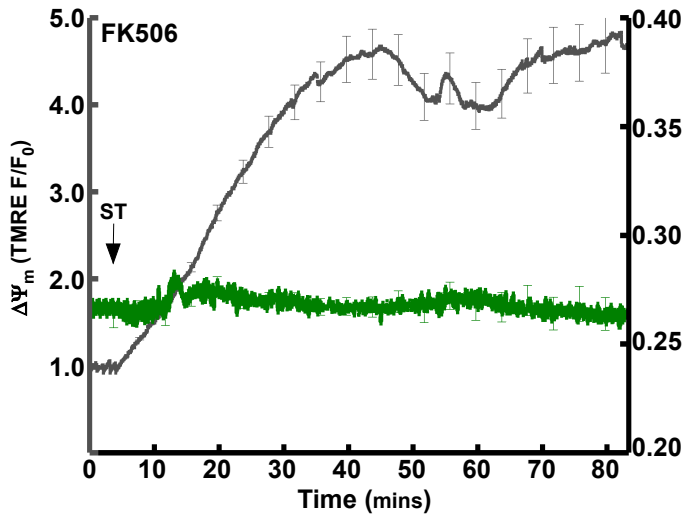


**Fig. S1 Related to Fig. 1: Spontaneous and stimulated permeability transition pore events underpin the intra and extra mitochondrial features of mitochondrial flickers** **A**, Live-cell imaging of control (Ctrl, upper) and Staurosporine-treated (ST, lower) HepG2 cells labeled with TMRE. Mean time course of TMRE calculated for all the recordings is plotted in Fig 1F. **B**, Difference image analysis of individual mitochondrial flicker in ST-stimulated HepG2 cells. Loss (Red) and recovery (Blue) of TMRE fluorescence used to monitor  $\Delta\psi_m$  over time. Flicker kinetic (lower right) derived from region of interest (ROI) restricted to active mitochondria. **C**, Box plot of mitochondrial flicker amplitude (Pre-flicker  $F_{TMRE} - F_{min}$ ) in control or ST-challenged cells (Ctrl, open. ST, Red hatching). **D**, Box plot of mitochondrial flicker duration in control cells (Ctrl, open) or oligomycin-treated cells (Oligo, 2.5 $\mu$ g/ml. Red hatching). **E**, Box plot of mitochondrial flicker duration (time of 1/2 max depolarization) in control or ST-challenged cells (Ctrl, open. ST, Red hatching) **F**, Frequency (mHz/cell) x Duration (time 1/2 max fluorescence) plot of individual mitochondrial flickers following ST addition (arrow). Mean  $\pm$  SEM. **G**, Examples of matrix pH (SypHer, Black) fluctuations during single, repeat, burst and sustained mitochondrial flickers (TMRE, dark red). **H**, Average trace of matrix pH within individual mitochondria during transient (left) and sustained (center) flickers (Mean  $\pm$  SEM, events synchronized to 1/2 max depolarization). Recovery kinetics of pH synchronized to peak were used to create best fit curves for transient (right, black exponential) and sustained (right, grey logistic) mitochondrial flickers. **I**, Histogram plot of matrix pH response duration (full width at half-maximum, FWHM). **J**, XY scatter plot of pHlash duration (at half-maximum) vs. Time. Pearson's and Spearman's rank correlations computed, ( $r$  = correlation coefficient). **K**, Box plot of pH increase duration vs iteration (number of pH events in a single mitochondrion within 600 s). Scale bars 5 $\mu$ m.

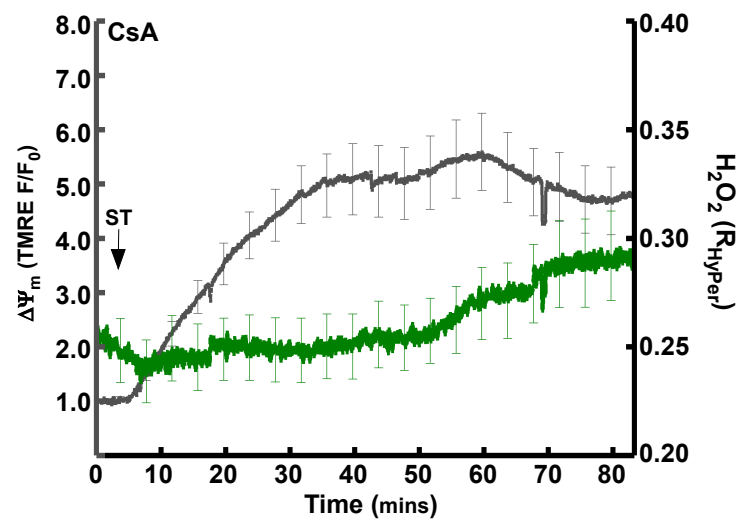
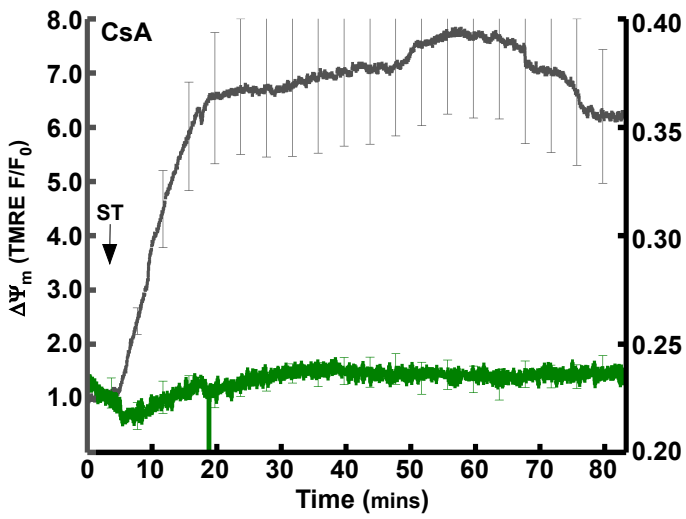
**A**

**B**

**C**

**D**

**E**

**F**

**G**

**H**

**I**


**Fig. S2 Related to Fig. 2: Mitochondrial flickers generate dynamic redox signals at the ER-mitochondrial interface.** **A**, Schematic representation of the mechanism used to target Grx1roGFP2 (green) to the ER-mitochondrial interface. We coupled the OMM and ER targeting sequences with the two components of the FKBP-FRB heterodimerization system and Grx1roGFP2 to each. Addition of rapamycin causes heterodimerization between adjacent FKBP and FRB domains to rapidly connect the ER- and OMM targeted anchors. Induction of the bridge formation is initially confined to the areas where the ER and OMM were naturally close. Thus, the probe-containing fusion proteins are concentrated at the ER-mitochondrial contacts via heterodimerization induced by a pulse of rapamycin (black). **B**, Box plot of flicker frequency in control (Untransfected) conditions or in cells expressing ER-M Grx1roGFP2 and OMM Grx1roGFP2 (Interface Grx1roGFP). Both Untransfected and Interface Grx1roGFP2 were subject to rapamycin pulse/FK506 protocol. **C**, Box plot of the dynamic range (Ratio maximum; oxidized with 200 $\mu$ M H<sub>2</sub>O<sub>2</sub>/Ratio minimum; fully reduced with 5mM DTT) of Grx1roGFP2 when targeted to subcellular compartments. Cytosolic face of ER: ER-M. Cytosolic face of the outer mitochondrial membrane (OMM), mitochondrial matrix (Matrix) and ER-M & OMM pairs targeted to the interface with rapamycin pulse/FK506 protocol. Both matrix and interface Grx1roGFP2 were measured with mitochondria polarized or depolarized with FCCP & Oligo (FCCP; 10 $\mu$ M & Oligomycin; 2.5 $\mu$ g/ml). **D**, Example traces of whole-cell oxidation of Interface Grx1roGFP2 following global depolarization of the mitochondrial network in 3 cells. **E, C**, plots of redox poise (GSSG:GSH) measured with Interface-targeted Grx1roGFP1 during the application of ST, following pre incubation with cyclosporine A (CsA; 5 $\mu$ M (Red)) or FK506 (FK506; 5 $\mu$ M (Green)) Plots are Mean  $\pm$  SEM. **F**, Examples of interface oxidative burst (Grx1roGFP2, green) activity during single, repeat, burst and sustained mitochondrial flickers stimulated by ST, respectively (TMRE, dark red). **G**, Histogram plot of interface oxidative burst duration (full width at half-maximum, FWHM). **H**, Box plots of individual interface GSSG:GSH peak durations vs iteration (number of GSSG:GSH peak events within 600 s) Relationship between iteration and oxidative burst duration significant (Chi Square 4-degrees of freedom,  $P < 0.001$ ). **I**, Box plots of interface GSSG:GSH (Grx1roGFP2,  $R-R_{\min}/R_{\max}$ ) at baseline (Grx1roGFP2, green) and peak (orange). Relationship between iteration vs. baseline, iteration vs. peak and iteration vs.  $\Delta$ GSSG:GSH (iteration peak-iteration baseline) all significant. (Chi square, 4-degrees of freedom,  $P < 0.001$ ).

**A**



**B**



**Fig S3 Related to Fig. 3 Mitochondrial flickers promote local Ca<sup>2+</sup> signals via oxidation of the IP<sub>3</sub>R. A,** Normalized recordings of  $\Delta\psi_m$  (TMRE; Black) and IP<sub>3</sub>R pH (Left, SypHer-IP<sub>3</sub>R1) and H<sub>2</sub>O<sub>2</sub> (Right, HyPer-IP<sub>3</sub>R1) levels during induction of flickers with ST following pre-incubation with 5 $\mu$ M FK506. **B,** Normalized recordings of  $\Delta\psi_m$  (TMRE; Black) and IP<sub>3</sub>R pH (Left, SypHer-IP<sub>3</sub>R1) and H<sub>2</sub>O<sub>2</sub> (Right, HyPer-IP<sub>3</sub>R1) levels during induction of flickers with ST following pre-incubation with 5 $\mu$ M cyclosporine A (CsA; 5 $\mu$ M).

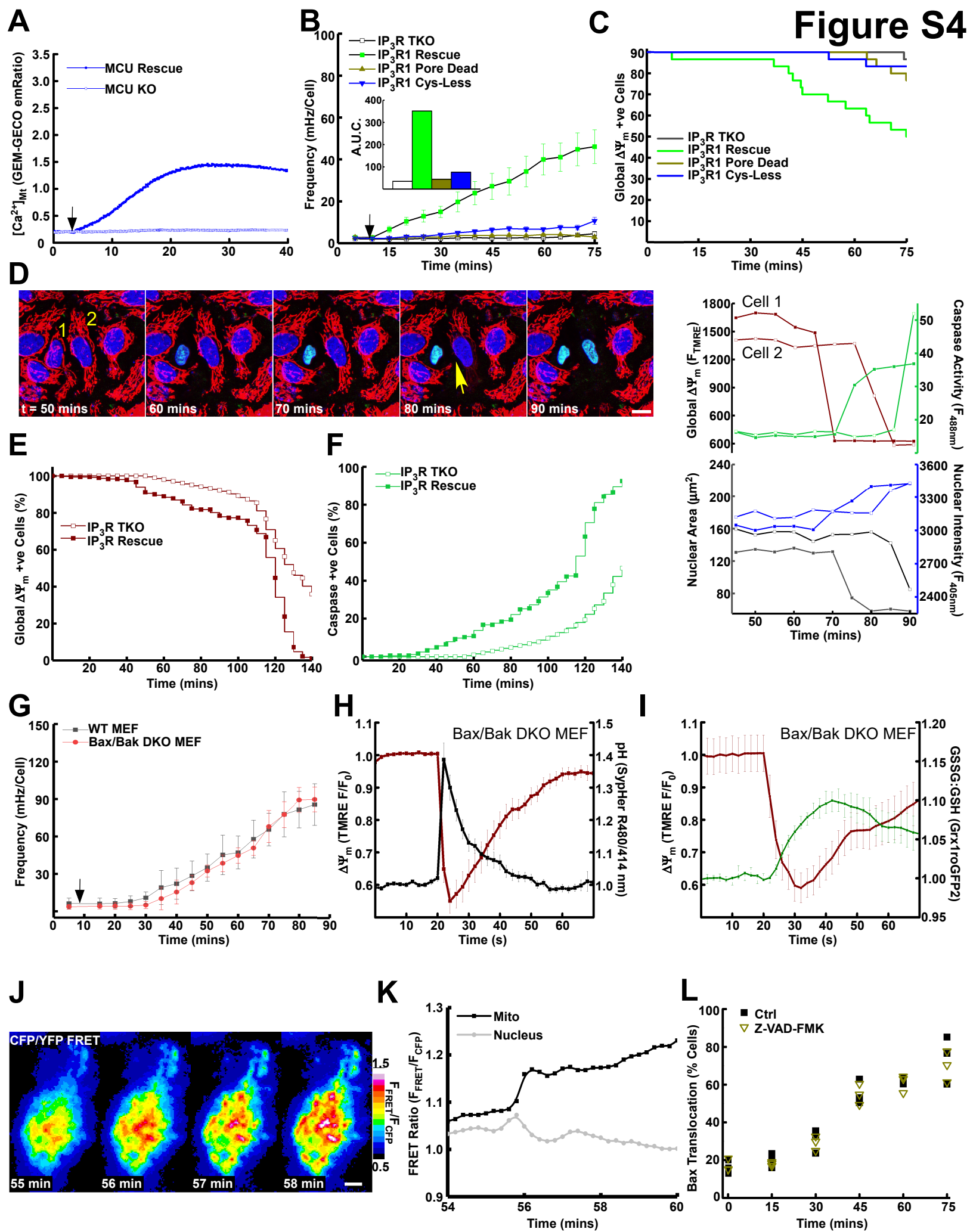


**Fig. S4 Related to Fig. 4: Mitochondrial flicker activity interacts with ER-mitochondrial  $\text{Ca}^{2+}$  transport.** **A**, Representative traces showing changes in  $[\text{Ca}^{2+}]_{\text{Mt}}$  assessed with expression of the emission ratiometric  $\text{Ca}^{2+}$  sensor GEM-GECO targeted to the mitochondrial matrix ( $[\text{Ca}^{2+}]_{\text{Mt}}$ : GEM-GECO Emission Ratio) in MCU KO (empty) and MCU Rescue (filled) cells. **B**, Flicker frequency (Mean  $\pm$ SEM) in HEK293T cells deficient in all 3 isoforms of the  $\text{IP}_3$  Receptor ( $\text{IP}_3\text{R-TKO}$ ; Black) Vs. Cells rescued with  $\text{IP}_3\text{R1}$  variants, WT  $\text{IP}_3\text{R1-mCherry}$  (Green;  $\text{IP}_3\text{R1-Rescue}$ ),  $\text{IP}_3\text{R1}$  mutated to prevent  $\text{Ca}^{2+}$ -flux ( $\text{IP}_3\text{R1-Pore Dead}$ ; Green), or  $\text{IP}_3\text{R1}$  deficient in cytosolic cysteine residues ( $\text{IP}_3\text{R1-CysLess}$ ; Blue). **C**, Kaplan-Meier plots of cell survival indicated by permanent global depolarization of mitochondrial  $\psi_m$  in  $\text{IP}_3\text{R-TKO}$  (Black),  $\text{IP}_3\text{R1-Rescue}$  (Green),  $\text{IP}_3\text{R1-Pore Dead}$  (Gold) and  $\text{IP}_3\text{R-Cys-Less}$  (Blue). **D**, Image sequence of apoptotic sequence in HepG2 cells treated with Staurosporine.  $\Delta\psi_m$  stained with TMRE; Red. Nucleus, Hoechst 33342; Blue and caspase 3/7 activation, Cell Event; Green. Cells labelled, #1 & 2 show sequential depolarization of  $\Delta\psi_m$ , (Red, traces: upper, Red) condensation and brightening of the nucleus, (Blue, traces: lower Black/Blue) and activation of executioner caspases 3/7 (Green, traces: upper Green). Global wave of  $\Delta\psi_m$  depolarization illustrated in image 4 with arrow indicating direction of wave. **E**, Kaplan-Meier plots of cell survival indicated by permanent global depolarization of mitochondrial  $\psi_m$  in  $\text{IP}_3\text{R-TKO}$  (Open),  $\text{IP}_3\text{R1-Rescue}$  (Closed). **F**, Plots of cell population in (E) assayed for executioner caspase activation (Caspase 3/7, Cell Event +ve nuclei). **G**, Flicker frequency in wild-type (WT-MEF; Black) and Bax/Bak double KO (Bax/Bak DKO MEF; Red) mouse embryonic fibroblasts during stimulation with Staurosporine (ST;  $2\mu\text{M}$ ). **H**, Average traces of transient mitochondrial flickers (Mean  $\pm$ SEM, dark red) and matrix pH rises (Mean  $\pm$ SEM, black) in mouse embryonic fibroblasts with double genetic targeting of bax & bak (Bax/Bak DKO MEF). **I**, Average traces of transient mitochondrial flickers (Mean  $\pm$ SEM, dark red) and matrix redox bursts (Mean  $\pm$ SEM, green) in Bax/Bak DKO MEF cells. Recordings synchronized to  $\frac{1}{2}$  max  $\Delta\psi_m$  depolarization. **J**, FRET images (CFP-YFP) of ST-treated HepG2 cells expressing both CFP-Bax & YFP-Bax during terminal  $\Delta\psi_m$  depolarization. **K**, FRET traces of two regions of interest, nucleus (Nucleus, light grey) and mitochondrial region (Mito, black) of the cell depicted in D. **L**, Plot of Bax oligomerization/translocation assay of ST treated HepG2 cells in the presence (empty yellow triangles) and absence (filled black squares) of a pan-caspase inhibitor (Z-VAD-FMK). Data derived from three independent experiments plotted for each time point. Scale bars  $5\mu\text{m}$ .